

Interplay of orbitally polarized and magnetically ordered phases in doped transition metal oxides

Raymond Frésard¹, Marcin Raczkowski^{1,2}, and Andrzej M. Oleś²

¹ Laboratoire CRISMAT, UMR CNRS-ENSICAEN (ISMRA) 6508, Caen, France

² Marian Smoluchowski Institute of Physics, Jagellonian University, Reymonta 4, 30059 Kraków, Poland

Key words two-band Hubbard model, magnetic order, orbital polarization, phase diagram.

PACS 75.10.-b, 75.10.Jm, 71.27.+a

We investigate the magnetic instabilities of the two-dimensional model of interacting e_g electrons for hole doping away from two electrons per site in the mean-field approximation. In particular, we address the occurrence of orbitally polarized states due to the inequivalent orbitals, and their interplay with ferromagnetic and antiferromagnetic spin order. The role played by the Hund's exchange coupling J_H and by the crystal field orbital splitting E_z in stabilizing one of the competing phases is discussed in detail.

Copyright line will be provided by the publisher

1 Introduction The richness of cooperative phenomena encountered in transition metal oxides continues attracting considerable attention. In addition to the spin and charge degrees of freedom, also the coupling to the lattice and, in particular, the orbital degrees of freedom at and close to the orbital degeneracy lead to very interesting behavior [1]. Here we will focus on the phenomena observed in nickelates and manganites, which can be attributed to strongly correlated e_g electrons. So far, it is known that in the regime of large intraorbital Coulomb interaction U strong quantum fluctuations may lead to qualitatively new behavior in a Mott insulator with three e_g electrons per site [2], but the competition between various magnetic and orbital instabilities was little explored in the weak coupling regime.

While several features are generic in the models with two [3] or more [4] orbitals per ion, and occur already when diagonal hopping is assumed, we note that these models are closer to the behavior of t_{2g} electrons — strong interactions between them might explain a ferromagnetic (FM) instability in ruthenates [5]. In contrast, the orbital flavor for e_g electrons is not conserved, and this is likely to lead to partial orbital polarization which is expected to modify the magnetic instabilities. Here we will consider such a realistic two-dimensional (2D) model of e_g electrons with (dd) hopping element t at intermediate and strong coupling, which includes the full structure of on-site Coulomb interactions with two parameters: the Hubbard element U and Hund's exchange J_H [6], and the crystal field orbital splitting E_z .

The magnetic and orbital instabilities within the e_g band were less investigated until now, but they become very relevant in the context of doped $\text{La}_{2-x}\text{Sr}_x\text{NiO}_4$ nickelates, where interesting novel phases including the stripe order were discovered [7]. They were obtained in the theory using realistic models both in Hartree-Fock [8] and in exact diagonalization of finite clusters including the coupling to the lattice [9]. Furthermore, the role of Hund's exchange in the FM instability and in the metal-insulator transition was emphasized using a multiband Gutzwiller wave-function [10]. All these studies reveal interesting competition between FM and antiferromagnetic (AF) instabilities at density $n = 1$, and the competition between the latter two and a C-AF instability at $n = 1.5$. In this paper we investigate the pure electronic problem for e_g electrons, using the mean-field approximation, seeking for phases which are both orbitally and magnetically polarized. By varying the electron density n between half filling $n = 2$ and $n = 0$, we cover the hole doping regime $x = n - 2$ relevant to the nickelates.

Corresponding author: e-mail: Raymond.Fresard@ensicaen.fr, Phone: +33 231 452 609, Fax: +33 231 951 600

2 Model In this work we consider a two-dimensional (2D) model for e_g electrons on a square lattice,

$$H = H_{\text{kin}} + H_{\text{int}} + H_z; \quad (1)$$

with two orbital flavors: $x^2 - y^2$ and $3z^2 - r^2$. The kinetic energy is described by

$$H_{\text{kin}} = \sum_{\langle ij \rangle} \sum_{\sigma} t_{ij} c_{i\sigma}^\dagger c_{j\sigma}; \quad t_{ij} = \frac{t}{4} \left(\frac{3}{2} \text{ for } \langle ij \rangle \parallel \hat{x} \text{ or } \hat{y}, \frac{1}{2} \text{ for } \langle ij \rangle \parallel \hat{z} \right); \quad (2)$$

where t stands for an effective (dd) hopping matrix element due to the hybridization with oxygen orbitals on Ni–O–Ni bonds, and the off-diagonal hopping t_{ij}^{xz} along a and b axis depends on the phase of the $x^2 - y^2$ orbital along the considered cubic direction. The electron-electron interactions are described by the on-site terms, which we write in the following form [6],

$$H_{\text{int}} = \sum_i U n_{ix} n_{ix\#} + n_{iz} n_{iz\#} + \sum_i \frac{5}{2} J_H n_{ix} n_{iz} + \sum_i 2J_H \mathbf{S}_{ix} \cdot \mathbf{S}_{iz} + \sum_i J_H c_{ix}^\dagger c_{ix\#}^\dagger c_{iz\#} c_{iz} + c_{iz}^\dagger c_{iz\#}^\dagger c_{ix\#} c_{ix}; \quad (3)$$

with $n_i = \sum_{\sigma} n_{i\sigma}$ (for $\sigma = x, z$). U and J_H stand for the intraorbital Coulomb and Hund's exchange elements. The interactions H_{int} are rotationally invariant both in the spin and in the orbital space. The last term H_z describes the uniform crystal-field splitting between $x^2 - y^2$ and $3z^2 - r^2$ orbitals,

$$H_z = \frac{1}{2} E_z \sum_i (n_{ix} - n_{iz}); \quad (4)$$

It is convenient to rewrite the Hamiltonian (3) by introducing the following operators:

$$n_i = \sum_{\sigma} n_{i\sigma}; \quad (5)$$

$$m_i = \sum_{\sigma} \sigma n_{i\sigma}; \quad o_i = \sum_{\sigma} \sigma n_{i\sigma}; \quad p_i = \sum_{\sigma} \sigma n_{i\sigma}; \quad (6)$$

$$f_i = \sum_{\sigma} c_{i\sigma}^\dagger \sigma c_{i\sigma}; \quad (7)$$

with $\sigma = 1$ for $\sigma = \#$ spin and $\sigma = 1$ for $\sigma = x(z)$ orbital, and σ is a Pauli matrix. These operators correspond to the total density, the total magnetization, the orbital polarization, the magnetic orbital polarization, and the on-site orbital flip respectively. The Coulomb interaction term H_{int} (3) can be then written as:

$$H_{\text{int}} = \frac{1}{8} \sum_i (3U - 5J_H) n_i^2 + (U + J_H) m_i^2 + (U - 5J_H) o_i^2 + (U - J_H) p_i^2 + \sum_i J_H f_i f_{i\#}; \quad (8)$$

The order parameters introduced in Eqs. (6): m_i , o_i , and p_i , used next to minimize the ground state energy, provide a complete description of the ground state at finite doping. We emphasize that they also reveal the dominating role of the kinetic energy of doped holes over the superexchange energy. Namely, large electron filling of $x^2 - y^2$ orbitals, contributing to a narrow band, optimizes the kinetic energy of holes in magnetically polarized states, doped into the $3z^2 - r^2$ orbitals, contributing to a wide band. On the contrary, the superexchange / $J = 4(t^x)^2/U$ at large U suggests that the system would better optimize the magnetic energy when the orbitals with larger hopping elements t^{xx} are closer to half filling. We show below that

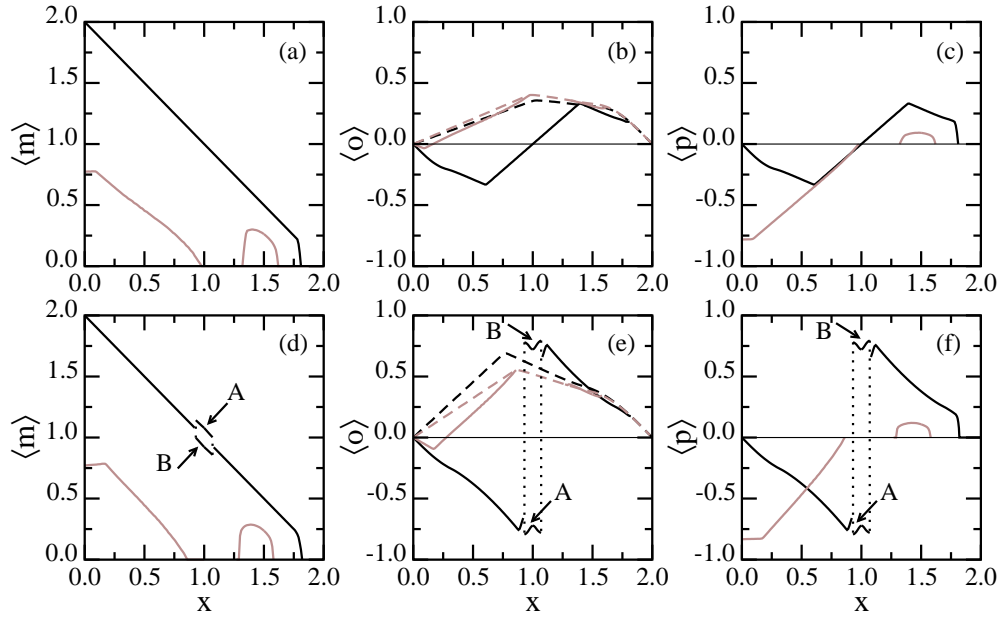


Fig. 1 Order parameters: magnetization $\langle m \rangle$, orbital polarization $\langle o \rangle$, and magnetic polarization $\langle p \rangle$ in the FM phase as a function of doping x for: (a)-(c) $J_H = 0.25U$ and (d)-(f) $J_H = 0.15U$, and for two values of the Stoner parameter: $U + J_H = 8t$ (black solid lines) and $U + J_H = 4t$ (gray solid lines). A and B refer to two sublattices in the orbital ordered state for $x = 1$. The orbital polarization in the reference PM states is shown by dashed lines.

the complex interplay between all the degrees of freedom of the model (1) results in rather peculiar doping dependence of the order parameters (6), and thus leads to highly nontrivial and rich phase diagrams.

We investigated the stability of possible phases with either uniform or staggered magnetic order in the mean-field (Hartree) approximation by expressing the local operators (6) by their mean-field averages, $\hat{c}_i^\dagger \hat{c}_i \approx \langle c_i^\dagger c_i \rangle + 2 \langle c_i \rangle \hat{c}_i - \langle c_i \rangle^2$. In order to establish unbiased results, the calculations were carried out on a large 128×128 cluster, using periodic boundary conditions at low temperature $T = 0.01t$ (here $k_B = 1$). Consistently with the present mean-field analysis we assumed $\hbar f_i = 0$.

3 Numerical results

3.1 Magnetic order and orbital polarization: First of all, in the paramagnetic (PM) state at $E_z = 0$, with $\langle m \rangle = \langle p \rangle = 0$, a higher electron density is found in χ -orbitals ($\langle o \rangle > 0$), as then the kinetic energy is lowered [Figs. 1(b) and 1(e)], except at $x = 0$. This state is our reference state for possible magnetic instabilities.

We now proceed with the discussion of the magnetic order and orbital polarization for two characteristic values of the Stoner parameter $I = U + J_H$: intermediate coupling $I = 4t$, and strong coupling $I = 8t$, being smaller and larger than the bandwidth $W = 6t$, respectively. Let us begin with the FM phase. In Fig. 1(a) we show the magnetization $\langle m \rangle$ as a function of doping x for the ratio $J_H/U = 0.25$ which is representative of the strong Hund's exchange coupling regime. In this case the interaction in the σ -channel is *repulsive*. As shown in Fig. 1, several FM phases occur.

Consider first the intermediate interaction strength $I = 4t$ [Figs. 1(a-c)], where one finds two disconnected FM states: one for $0 < x < 1$, and the second one for $x > 1.5$. The latter corresponds to a van Hove singularity in the density of states. Since it is predominantly related to the χ -orbital, both the orbital polarization $\langle o \rangle$ [Fig. 1(b)] and the magnetic polarization $\langle p \rangle$ [Fig. 1(c)] are positive in this doping regime.

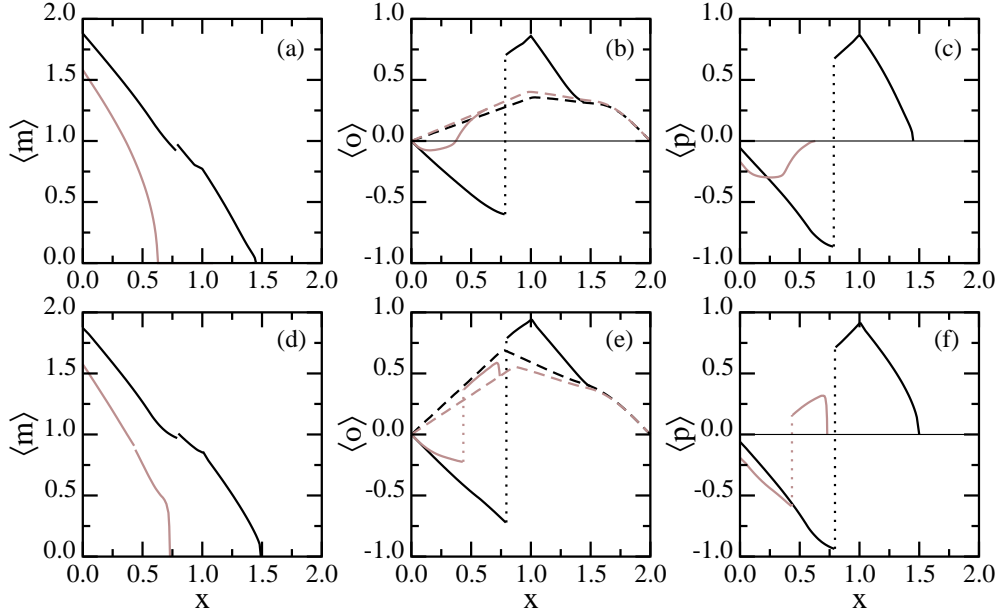


Fig. 2 Order parameters as in Fig. 1 but for the AF phase.

In contrast, for $0 < x < 1$ the total energy is minimized when a higher electron density is found in the $\bar{x}i$ orbital, where also larger magnetic moments are formed. Such anisotropic filling of e_g orbitals follows from a large difference between the t^{xx} and t^{zz} hopping elements [11]. Note that the orbital polarization is here opposite to that in the reference PM state.

The above peculiar behavior disappears gradually when the interaction strength is enhanced to $I = 8t$ and both $\langle o_i \rangle$ and $\langle p_i \rangle$ tend to saturate to the optimal value, being positive (negative) for $x < 1$ ($x > 1$), leaving the $\bar{x}i$ orbital almost fully polarized. Here the magnetic instability, with the largest effective interaction term $U + J_H$, dominates and the magnetization barely deviates from its saturation value $2 - x$, except for the low electron density $x > 1.3$. In this case doping the half-filled FM state first leads to holes introduced into the $\bar{x}i$ orbitals, leaving the center of the narrower band, with predominantly $\bar{x}i$ orbital character, below the former broader one. Therefore, in this situation the formation of localized magnetic moments optimizes the energy. They are naturally associated with the $\bar{x}i$ orbitals since they contribute to the narrower band.

When Hund's exchange coupling J_H is reduced, the interaction in the o -channel becomes *attractive*. As a result, for large $I = 8t$, both $\langle o_i \rangle$ and $\langle p_i \rangle$ nearly saturate to the ideal behaviors $-x$ for $x < 1$ and $2 - x$ for $x > 1$. Therefore, a transition between these two solutions would be first order, and one observes a jump at $x = 1$. However, as shown in Figs. 1(d-f), the two-sublattice orbital order sets in in this crossover regime in the form of a FM_{xz} state. This state has opposite orbital polarization $\langle o_{iA} \rangle = 0.3$ and $\langle o_{iB} \rangle = 0.3$ on both sublattices [Fig. 1(e)]. While the total density $\langle m_{iA} \rangle$ is somewhat higher than $\langle m_{iB} \rangle$ due to inequivalent e_g orbitals, also $\langle m_{iA} \rangle > \langle m_{iB} \rangle$. For large doping $x > 1$ the electrons occupy mainly the $\bar{x}i$ orbitals, and the small occupancy of $\bar{x}i$ orbital results solely from the interorbital hopping term t_{xz} . Indeed, at $x = 1.3$ one finds appreciable orbital polarization, with $\bar{x}i$ orbitals occupied and almost empty $\bar{x}i$ orbitals, the situation encountered in $La_{1-x}Sr_{1+x}MnO_4$ manganites [12]. In all FM phases found at $J_H = 0.15U$ the total magnetization is close to saturation. When U is reduced, one gradually recovers the behavior obtained for large $J_H = U$.

We now turn to the AF phase, expected as a ground state near half filling ($x = 0$). The order parameters are shown in Fig. 2 for the same parameter values as for the FM case. For $I = 8t$ and $J_H = U = 0.25$ the

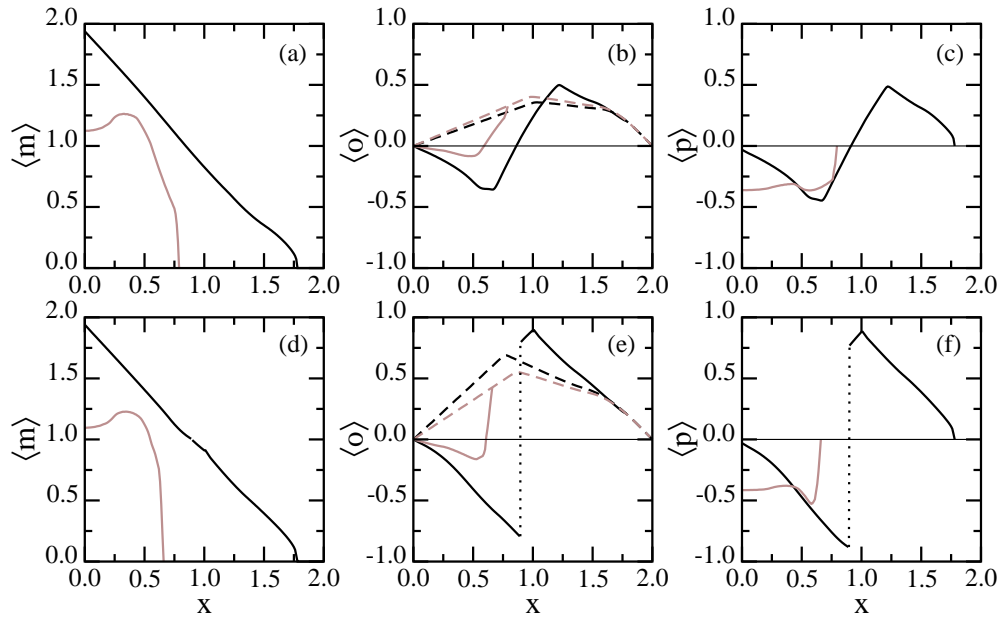


Fig. 3 Order parameters as in Fig. 1 but for the C-AF phase.

mean-field equations possess two competing solutions [Figs. 2(a-c)]. The first one, which can be continued to weak coupling, is characterized by negative values of orbital $\langle o \rangle$ and magnetic $\langle p \rangle$ polarizations. Namely, the higher electron density is found within the $\downarrow\uparrow$ orbitals, and these orbitals carry the magnetic moment. More precisely, introducing holes in the half-filled insulating AF state mostly affects the band with $\downarrow\uparrow$ orbital character, leaving the localized magnetic moments within the $\downarrow\uparrow$ orbital almost saturated. This solution extends to large doping $x \rightarrow 1$. In contrast, the second solution rather stems from the behavior expected for low density: the electrons first occupy the broader band with $\downarrow\uparrow$ orbital character until quarter filling ($x = 1$) is reached, and next they gradually occupy the other band, with $\uparrow\downarrow$ orbital character. However, since the interaction in the o -channel is *repulsive* and since both bands are coupled, the orbital polarization $\langle o \rangle$ and the magnetic polarization $\langle p \rangle$ are reduced from their maximal values which would be reached for decoupled orbitals. These two trends from $x = 0$ and $x = 2$ contradict each other, and therefore an abrupt (first order) transition between both solutions is observed at $x \approx 0.7$ [Figs. 2(b-c)].

Reducing J_H barely affects the above findings for strong coupling $I = 8t$ [Fig. 2(d-f)]. While the magnetization $\langle m \rangle$ is almost unchanged, the first order transition between two differently polarized states is more pronounced, as the values of the orbital polarization and the magnetic polarization are enhanced. When reducing U the location of the first order phase transition shifts towards smaller doping, while all order parameters are suppressed. At the same time the critical doping locating the second order phase transition is reduced by a weaker Coulomb interaction U but is enhanced by a weaker Hund's exchange coupling J_H . When seeking for other phases one may expect that two-sublattice FM solutions can smoothly interpolate between the FM and AF states. Such solutions never turned out to be the ground state in this study (up to $I = 8t$).

A competition between the FM and AF order in the present model of e_g band may lead to a superposition of the two phases in a form of C-AF phase, where the magnetic moments are FM along one direction and staggered in the other (orthogonal) one. According to recent numerical simulations [9], a coexistence of FM and AF bonds is indeed expected for $x \approx 0.5$. Unlike in the AF phase, the order parameters are continuous functions of doping for $J_H = U = 0.25$, as can be seen in Figs. 3(a-c). This behavior is similar to that of the FM case (Fig. 1). Its origin can be attributed to the orbital polarization which is substantially

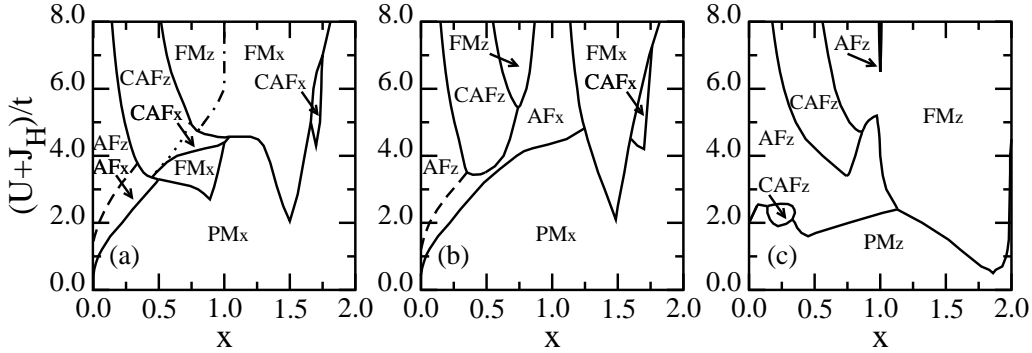


Fig. 4 Phase diagrams of the e_g orbital model (1) as functions of the Stoner parameter $U + J_H$ and hole doping $x = 2 - n$, with: (a) $J_H = 0.25U$, and (b) $J_H = 0.15U$. Panel (c) shows the stable phases for finite crystal field splitting $E_z = 2t$ and $J_H = 0.25U$. Transitions from the PM phase to magnetic phases are second order. The remaining solid lines denote first order transitions while the dashed, dotted, and dashed-dotted lines indicate second order transitions.

stronger in the AF case to the extent that it exceeds a certain threshold above which no smooth solution can interpolate between the small and large doping regimes. For $x < 0.5$ the magnetic moment m_i is carried by the $\bar{x}i$ orbital for large U , while m_i decreases and $\bar{h}i$ changes sign for small U .

When reducing $J_H = U$, the orbital polarization is enhanced and a first order transition appears for $I = 8t$ [see Figs. 3(d-f)]. In this case both the orbital polarization and the magnetic moment are predominantly carried by the stronger correlated $\bar{x}i$ orbital (with a weaker hopping and thus larger ratio $U = t^{\bar{x}z}$ than $U = t^{xx}$) in the physically relevant doping range centered around $x = 0.5$.

3.2 Magnetic phase diagrams: Our main findings are summarized in the phase diagrams in Fig. 4. For $J_H = U = 0.25$ [Fig. 4(a)], the doped PM phase is characterized by a positive orbital polarization, therefore denoted PM_x . It is unstable towards AF_x phase for small doping up to $x \approx 0.5$, towards $C-AF_x$ phase for $1 \leq x \leq 1.02$ and for $1.65 \leq x \leq 1.75$, and towards FM_x phase otherwise. In particular, for $x = 1$ the FM_x , $C-AF_x$, orbitally unpolarized FM and (for $I > 16t$) the alternating FM_{xz} phases appear successively with increasing interaction strength I . The $C-AF$ phases are found for $x \approx 0.5$ at $I > 4t$, and also in a small range around $x \approx 0.75$.

When reducing $J_H = U$ [Fig. 4 (b)], the main difference appears for $x \approx 1$. Here the PM_x phase is unstable towards an AF_x phase which itself is robust and remains stable up to strong coupling. This seemingly peculiar behavior can be better understood by diagonalizing exactly a two-site cluster. One can find the ground state to be AF_x for small J_H and arbitrary U and FM_{xz} for large $J_H = U$, in qualitative agreement with our mean-field calculation.

Let us finally mention that the model we use is known to have a van Hove singularity in the vicinity of $x = 1.5$, which is expected to induce a FM instability for arbitrary weak coupling at zero temperature. This particular instability, however, turns out to be unusually strongly temperature dependent. Therefore, the corresponding critical value of the Stoner parameter I is finite at temperature $T > 0$, and reaches a value close to $W \approx 3$ (Fig. 4) at $T = W \approx 600$ used in this work.

3.3 Consequences of the crystal field splitting: A complete investigation of the phase diagrams at finite crystal field splitting E_z would be quite involved, and is left for future work. At $E_z = 0$ the majority of stable magnetic solutions is characterized by a positive orbital polarization, a tendency expected for a 2D model of e_g electrons [12], which would certainly be enhanced by a negative crystal field E_z . We therefore limit our present discussion to the influence of a positive E_z , in order to investigate a competition between the kinetic energy, which is lower when the broad band with predominantly $\bar{x}i$ orbital character is closer

to half filling, and the potential energy at finite E_z . Furthermore, we restrict ourselves to the strong Hund's exchange coupling regime $J_H = 0.25U$.

As shown in Fig. 4(c), the orbital polarization of the PM phase is changed to negative (PMz phase) already for moderate $E_z = 2t$. As a result, the magnetic moment and the orbital polarization are carried by the same orbital in all phases, and the magnetic instabilities are achieved for lower values of $I = U + J_H$. Another consequence of finite $E_z > 0$ is the observed shift of the van Hove singularity to larger doping, strongly enhancing the tendency towards ferromagnetism in the low density regime. In addition, the competition between FM and AF phases at quarter filling ($x = 1$) remains quite spectacular: even though both weak coupling and strong coupling expansions predict antiferromagnetism, as does our calculation, FM phase nevertheless takes over in an intermediate coupling regime $5.15t < I < 6.5t$.

Such features as the AFz phase obtained for low doping, the C-AFz phase for $x = 0.5$, and FM one for both $0.5 < x < 0.98$ and $x > 1.02$, are robust and are found also at finite crystal field, in particular in the strong coupling regime. On the contrary, the instability of the PM phase to the FMx phase disappears, and the one to the C-AF phase moves from $x = 1.5$ to small doping.

4 Conclusions In summary, we have determined the phase diagram of e_g electrons on the square lattice within the mean-field approximation. The occurrence of antiferromagnetism in the vicinity of half filling, followed by C-AF phase at $x = 0.5$, as well as FM phases for $x = 0.75$ and $x = 1.5$, are robust features of this model. Note that the regions of stability of the AF and C-AF phases with respect to the FM one would still be somewhat extended due to quantum corrections [13]. In particular, the occurrence of C-AF phase indicates that even more complex types of magnetic phases, such as stripe phases with larger magnetic unit cells [7, 9], might be expected in doped nickelates.

In contrast, the ground state is strongly parameter dependent in the vicinity of quarter filling, $x = 1$, resembling to some extent the ground state of the model with two equivalent orbitals [3, 5]. While the orbital polarization systematically appears in all phases, the orbital carrying the magnetic moment does not necessarily coincide with the one carrying higher electron density, leading to a particularly interesting interplay between magnetic and orbital degrees of freedom.

Acknowledgements M. Raczkowski was supported by a Marie Curie fellowship of the European Community program under number HPMT2000-141. A. M. Oleś would like to acknowledge support by the Polish State Committee of Scientific Research (KBN) under Project No. 1 P03B 068 26.

References

- [1] S. Maekawa, T. Tohyama, S. E. Barnes, S. Ishihara, W. Koshibae, and G. Khaliullin, *Physics of Transition Metal Oxides* Springer Series in Solid State Sciences Vol. 144 (Springer Verlag, Berlin, 2004).
- [2] L. F. Feiner, A. M. Oleś, and J. Zaanen, *Phys. Rev. Lett.* **78**, 2799 (1997).
- [3] A. Klejnberg and J. Spalek, *Phys. Rev. B* **61**, 15542 (2000); L. Didukh, Yu. Skorenky, V. Hankevych, and O. Kramar, *Phys. Rev. B* **64**, 144428 (2001); A. Koga, Y. Imai, and N. Kawakami, *Phys. Rev. B* **66**, 165107 (2002); A. Koga, N. Kawakami, T. M. Rice, and M. Sgrist, *Phys. Rev. Lett.* **92**, 216402 (2004).
- [4] S. Florens, A. Georges, G. Kotliar, and O. Parcollet, *Phys. Rev. B* **66**, 205102 (2002); Y. Ōno, M. Potthoff, and R. Bulla, *Phys. Rev. B* **67**, 035119 (2003); S. Florens and A. Georges, *Phys. Rev. B* **70**, 035114 (2004).
- [5] R. Frésard and M. Lamboley, *J. Low Temp. Phys.* **126**, 1091 (2002).
- [6] A. M. Oleś, *Phys. Rev. B* **28**, 327 (1983).
- [7] J. M. Tranquada, J. E. Lorenzo, D. J. Buttrey, V. Sachan, *Phys. Rev. B* **52**, 3581 (1995); J. Li, Y. Zhu, J. M. Tranquada, K. Yamada, and D. J. Buttrey, *Phys. Rev. B* **67**, 012404 (2003).
- [8] T. Mizokawa and A. Fujimori, *Phys. Rev. B* **56**, 11920 (1997).
- [9] T. Hotta and E. Dagotto, *Phys. Rev. Lett.* **92**, 227201 (2004).
- [10] J. Bünemann, W. Weber, and F. Gebhard, *Phys. Rev. B* **57**, 6896 (1998).
- [11] J. Zaanen and A. M. Oleś, *Phys. Rev. B* **48**, 7197 (1993).
- [12] F. Mack and P. Horsch, *Phys. Rev. Lett.* **82**, 3160 (1999).
- [13] M. Raczkowski and A. M. Oleś, *Phys. Rev. B* **66**, 094431 (2002).